Top Catal (2016) 59:583–590
DOI 10.1007/s11244-015-0533-3

ORIGINAL PAPER

In-Situ Probing of H_2O Effects on a Ru-Complex Adsorbed on TiO_2 Using Ambient Pressure Photoelectron Spectroscopy

Susanna K. Eriksson[1] · Maria Hahlin[2] · Stephanus Axnanda[3] · Ethan Crumlin[3] · Regan Wilks[4,5] · Michael Odelius[6] · Anna I. K. Eriksson[1] · Zhi Liu[3] · John Åhlund[7] · Anders Hagfeldt[1] · David E. Starr[8] · Marcus Bär[4,5,9] · Håkan Rensmo[2] · Hans Siegbahn[2]

Published online: 20 January 2016

Abstract Dye-sensitized interfaces in photocatalytic and solar cells systems are significantly affected by the choice of electrolyte solvent. In the present work, the interface between the hydrophobic Ru-complex Z907, a commonly used dye in molecular solar cells, and TiO_2 was investigated with ambient pressure photoelectron spectroscopy (AP-PES) to study the effect of water atmosphere on the chemical and electronic structure of the dye/TiO_2 interface. Both laboratory-based Al Kα as well as synchrotron-based ambient pressure measurements using hard X-ray (AP-HAXPES) were used. AP-HAXPES data were collected at pressures of up to 25 mbar (i.e., the vapor pressure of water at room temperature) showing the presence of an adsorbed water overlayer on the sample surface. Adopting a quantitative AP-HAXPES analysis methodology indicates a stable stoichiometry in the presence of the water atmosphere. However, solvation effects due to the presence of water were observed both in the valence band region and for the S 1s core level and the results were compared with DFT calculations of the dye-water complex.

Keywords Dye-sensitized solar cells · AP-HAXPES · DFT · H_2O · Photoelectron spectroscopy

1 Introduction

Dye-sensitized interfaces have been extensively studied due to their important role in devices that convert solar to chemical energy, (e.g. in photocatalysis [1]) or to electrical energy (e.g. in dye-sensitized solar cells (DSCs)) [2–4]. Energy conversion in systems such as DSCs is based on the photoexcitation of a dye molecule adsorbed on a wide band-gap semiconductor and charge injection from the dye into the semiconductor. The oxidized dye is regenerated by a liquid electrolyte or a solid hole conductor. To date, Ru-based organometallic complexes are among the most extensively used dye molecules for DSCs.

The energy conversion process in electrolyte-based devices is strongly influenced by the choice of solvents. Water-based liquid electrolytes are particularly desirable

✉ Maria Hahlin
maria.hahlin@physics.uu.se

✉ Zhi Liu
zliu2@lbl.gov

1 Department of Chemistry-Ångström, Uppsala University, Box 523, 751 20 Uppsala, Sweden

2 Department of Physics and Astronomy, Uppsala University, Box 516, 751 20 Uppsala, Sweden

3 Advanced Light Source, Lawrence Berkeley National Laboratory, One Synchrotron Rd., Berkeley, CA 94720, USA

4 Renewable Energy, Helmholtz-Zentrum Berlin für Materialien und Energie GmbH, Hahn-Meitner-Platz 1, 14109 Berlin, Germany

5 Energy Materials In-Situ Laboratory (EMIL), Helmholtz-Zentrum Berlin für Materialien und Energie GmbH, Albert-Einstein-Str. 15, 12489 Berlin, Germany

6 Department of Physics, AlbaNova University Center, Stockholm University, 106 91 Stockholm, Sweden

7 VG Scienta AB, Box 15120, 750 15 Uppsala, Sweden

8 Institute for Solar Fuels, Helmholtz-Zentrum Berlin für Materialien und Energie GmbH, Hahn-Meitner-Platz 1, 14109 Berlin, Germany

9 Institut für Physik und Chemie, Brandenburgische Technische Universität Cottbus-Senftenberg, Platz der Deutschen Einheit 1, 03046 Cottbus, Germany

since water is abundant and environmentally friendly. The performance of purely water-based solar cells is however generally lower than state-of-the-art organic solvent electrolyte-based devices. The presence of water has a direct effect on the current–voltage characteristic of DSCs [5, 6]. Water has also been shown to accelerate device degradation and cause desorption of the dye molecules [7]. Even when an organic solvent is used, traces of water may still be present (as an impurity) and importantly, water often leaks into the device during long-term use. Introducing hydrophobic chains on the dye helps to alleviate these problems, but yet challenges still remain [5, 8]. A molecular-level understanding of the effect of water on the functional interface would greatly aid the development of efficient water-based DSCs but is still missing.

Photoelectron spectroscopy (PES) is a surface-sensitive characterization technique highly suited for studying surfaces and interfaces present in DSCs. PES studies of DSCs have typically been performed on dry electrodes under ultra-high vacuum conditions, including attempts to understand the interaction with solvent molecules [9–13]. In addition, complementary studies conducted on iodide electrolytes using a liquid jet system have been made [14, 15]. In previous work, the effect of water on Z907 dye molecules, with the hydrophobic ligand 4,4-dinonyl-2,2-bipyridine (cf. Fig. 1), was investigated using vacuum-based PES [12]. In that study, the dye-sensitized electrodes were exposed ex situ to ethanol/water solutions of various concentrations for 20 min and subsequently measured using PES under ultra-high vacuum conditions. For Z907-sensitized samples, this exposure gave no significant change in solar cell performance, while larger changes were observed for less hydrophobic Ru-based dye molecules. The conclusions were that the hydrophobic chains protect the Z907 dye molecule from detrimental structural changes upon water exposure and reduce the likelihood of it desorbing from the surface.

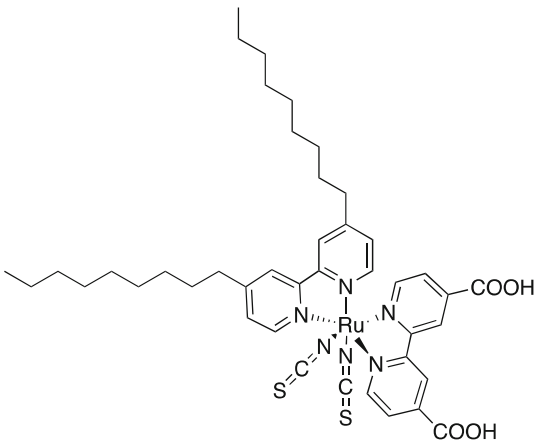

Fig. 1 The structure of the ruthenium based dye molecule Z907

The recent development of ambient pressure PES (AP-PES) has made in situ measurements possible in the presence of water vapor or even liquid water films [16–18]. AP-PES dates back to the efforts of Siegbahn and co-workers in the 1970s [19–21]. The technique has developed rapidly in recent years due to the use of differentially pumped electron lens systems in both synchrotron-based [22–26] and laboratory-based systems [27, 28]. One of the main challenges of AP-PES techniques is the scattering of the photoemitted electrons by the ambient gas phase molecules when the pressure is increased. The emitted photoelectrons will be attenuated, depending on their kinetic energy, compared to PES ultra-high vacuum experiments (usually performed below 10^{-8} mbar), which requires careful considerations in interpreting sample stoichiometries from photoelectron line intensities. Scattering effects can be reduced by increasing the kinetic energy of the photoelectrons, effectively increasing the inelastic mean free path of the photoelectrons. PES using higher photon energies is known as hard X-ray photoelectron spectroscopy (HAXPES). A combination of AP-PES measurements with hard X-rays (i.e. AP-HAXPES), is therefore ideal for in situ studies of TiO_2 supported dye molecules in the presence of elevated partial pressures of gaseous water or thin liquid films. In addition, with AP-HAXPES there is the possibility to see through liquid films of greater thickness, which enables the investigation of molecular solvation.

In this paper, we have used both a laboratory-based AP-PES system optimized for lower pressures (up to 2 mbar) [28] and a synchrotron-based AP-HAXPES setup optimized for higher pressures (up to 25 mbar), to study the effect of exposure to gaseous water up to pressures of 25 mbar (water vapor pressure at 22.2 °C) on the chemical and electronic structure of Z907 dye molecules adsorbed on TiO_2. The interaction between water and dye molecules was also modeled using density functional theory calculations (DFT) and the results compared to experimental data.

2 Methods

2.1 Sample Preparation

A layer of DSL 18 NR-T TiO_2 paste (purchased from Dyesol and used as received) was screen printed on top of F-doped tin oxide (FTO) conductive glass (Pilkington TEC 15). The substrates were heated for 5 min at 120 °C, sintered at 500 °C for 30 min and left to cool over night in air. This yielded a TiO_2 layer with thicknesses between 5 and 6 μm. Before sensitization, the electrodes were re-heated to

approximately 300 °C for 10 min and then cooled to about 80 °C. The dye solution was a 0.3 mM solution of *cis*-disothiocyanato(2,2-bipyridyl-4,4-dicarboxylic acid)-(2,2-bipyridyl-4,4-dinonyl)ruthenium(II) (Z-907, for structure see Fig. 1) dissolved in ethanol. For sensitization the TiO_2/FTO substrates were immersed in the Z907 containing solution for approximately 20 h. The samples were transferred into the measurement chambers immediately after sensitization leaving the samples in air less than 0.5 h.

2.2 Laboratory-Based AP-PES

The AP-PES measurements were performed with a system consisting of a Scienta R4000 HiPP-2 high pressure analyzer, a monochromatized Scienta MX650 HP Al Kα X-ray source, an analysis chamber, a load lock chamber and a manipulator, as previously described [28]. The X-ray monochromator is mounted at an angle of 62.5° with respect to the symmetry axis of the analyzer pre-lens. The pass energy of the analyzer was 200 eV. A 0.8 mm entrance aperture was used for the electron lens entrance which optimizes the signal intensity for gas pressures of around 2 mbar [28]. The swift acceleration mode was implemented to compensate for the lower kinetic energies of the electrons using Al Kα excitation, compared to the AP-HAXPES energies [29]. The water vapor was leaked into the analysis chamber from a test tube via two leak valves. To degas the water, the test tube was freeze-pumped three times.

2.3 Synchrotron-Based AP-HAXPES

The AP-HAXPES measurements were conducted at the bending magnet beamline 9.3.1 of the Advanced Light Source (ALS) at Lawrence Berkeley National Laboratory [30]. The end-station is equipped with a Scienta R4000 HiPP-2 spectrometer [31]. The angle between the photon polarization and photoelectron emission directions is 15° for this system. The photon energy used was 4000 eV and the pass energy was 200 eV. A 0.3 mm entrance aperture was employed allowing for measurements at water pressures up to 25 mbar of gaseous water. Pressure equilibrium was maintained by balancing the water vapor pumped out of the chamber through the electron energy analyzer's differential pumping system by leaking water into the chamber through a leak valve connected to a test tube containing liquid water. The water in the test tube was freeze-pumped twice before use. The measurement spot on the sample was frequently changed to minimize the effects of radiation damage on the spectra collected. The binding energies of all spectra were calibrated versus the substrate Ti $2p_{3/2}$ peak binding energy (458.56 eV) according to previous measurements [9].

2.4 Density Functional Calculations

Core level binding energies for a Z907 model structure with aliphatic chains truncated to ethyl groups interacting with water were simulated with density functional theory (DFT) to investigate how water coordination influences the S 1s binding energies. In the Gaussian code [32], complexes of the 4,4-diethyl-2,2-bipyridine analogue of Z907 with one and two water molecules were optimized using the B3LYP [33] hybrid density functional and (LanL2DZ) Los Alamos effective core potentials with DZ basis sets for sulfur and ruthenium [34] and D95V basis sets on remaining elements [35]. Several configurations were investigated, of which a subset for the coordination at the NCS ligands and carboxyl groups is presented. Subsequently in the StoBe code [36], S 1s core level binding energies were obtained as the total energy difference between the ground and core-ionized states using gradient corrected exchange and correlation functionals [37, 38] with the III iglo basis set [39] on sulfur, a DZVP(PNW) basis set on Ru and TZVP(PNW) basis sets on the remaining atoms [40]. An auxiliary basis set for density fitting was generated from the corresponding orbital basis using the GENA3 procedure.

3 Results and Discussion

In Fig. 2a, O 1s spectra of the dye-sensitized TiO_2 sample are shown in vacuum and at two different water vapor pressures (11 mbar and 25 mbar). The spectra were measured with a photon energy of 4000 eV and normalized to the substrate TiO_2 O 1s contribution. The vacuum spectrum contains a contribution on the high binding energy side of the substrate peak due to the oxygens of the dye. With elevated pressures a strong gaseous water peak appears at 536.4 eV. As can be seen, with increasing water pressure additional intensity is observed at around 533 eV. We attribute this observation to water condensing on the sensitized TiO_2 substrate with increasing pressure of gaseous water in the analysis chamber. Figure 2b shows a subtraction of the vacuum spectrum from the 25 mbar spectrum, indicating a binding energy difference between this new O 1s contribution and the O 1s peak of gaseous water of approximately 3 eV, which is in accordance with water adsorbed on an organic material [41]. We estimate from the relative intensity of this water signal that the layer is not in liquid form, but rather present in terms of specifically adsorbed species or clusters.

Carbon, ruthenium, nitrogen, and sulfur core-levels can be used to study the influence of water on the chemical structure of the dye molecule. Specific effects on the NCS ligands (see Fig. 1) are studied here using the S 1s signal, since its higher photoionization cross section at 4000 eV

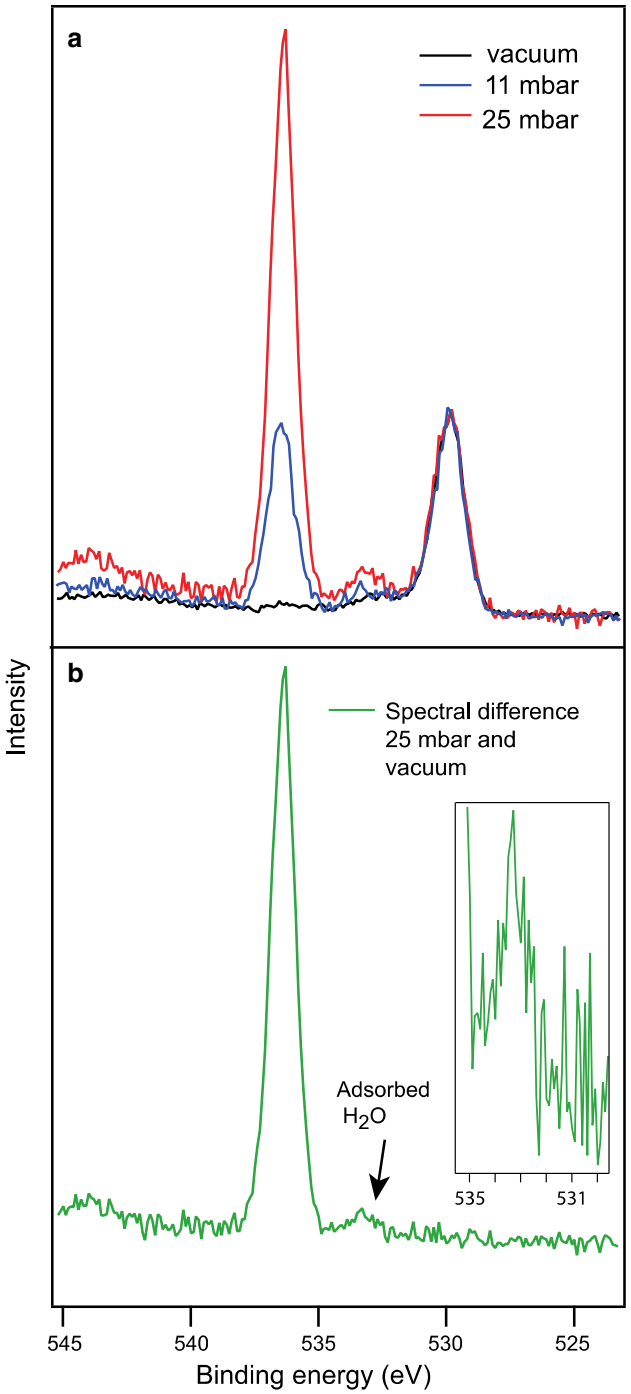

Fig. 2 **a** O 1s spectra of the dye-sensitized TiO_2 samples recorded at different pressures of water vapor with 4000 eV at the ALS beamline 9.3.1. The spectra are intensity normalized to the O 1s substrate peak at 530 eV. The peak at higher binding energy (536.2 eV) is ascribed to oxygen in the gaseous water molecules. A small feature around 533 eV appears at higher pressures (above 11 mbar), due to formation of adsorbed water. **b** The same data as in figure **a** where the vacuum data has been subtracted from 25 mbar data to highlight the signal due to adsorbed water (*inset* with a magnification of a factor ten)

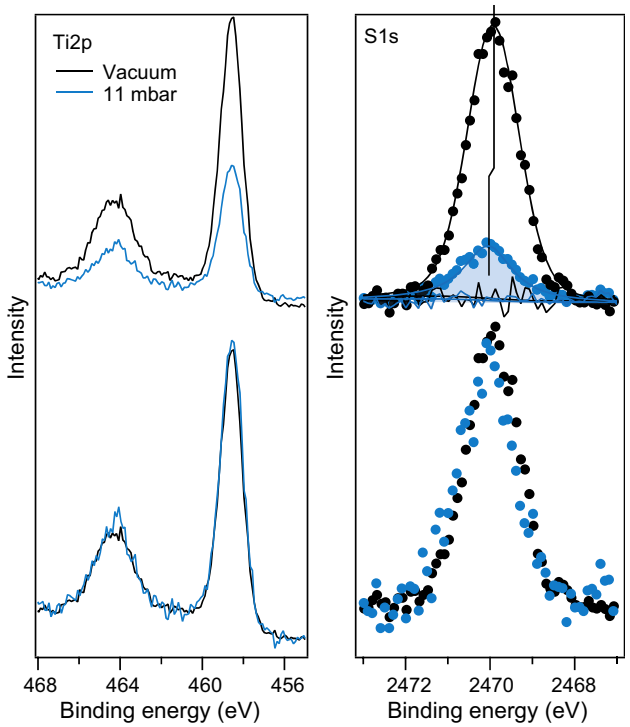

Fig. 3 Ti 2p and S 1s spectra measured of the dye-sensitized TiO_2 with an excitation energy of 4000 eV. The upper Ti 2p and S 1s spectra are normalized to measurement time revealing a substantial attenuation of intensity at higher pressures. The lower Ti 2p and S 1s spectra were corrected for attenuation according to Eq. 1 due to electron scattering caused by the ambient H_2O molecules

(compared to that of the S2p level) makes it easier to detect. The corresponding Ti 2p spectra are shown along with the S 1s spectra in Fig. 3. The scattering of electrons by gas molecules depends on the kinetic energy of the photoelectrons, and so the attenuation of the intensity differs significantly for the Ti 2p and S 1s core levels. This is clearly seen when comparing spectra that have been corrected for differences in the attenuation to those without correction. In the upper part of Fig. 3, the intensities are normalized to measurement time. In the lower part of Fig. 3, the intensities are adjusted for electron scattering by gas-phase water. The attenuation at different pressures is described by Eq. 1 [16],

$$I_p = I_0 \exp\left(-z\sigma p/kT\right) \quad (1)$$

where I_p and I_0 are the intensities at pressure p and in vacuum, respectively. The electron scattering cross sections (σ) were obtained from reference 41 (σ (1530 eV) and σ (3540 eV) equal to 1.14×10^{-20} and 5.99×10^{-21} m^2, respectively) [42] and z is estimated to be 0.5 mm (the distance the electron has to travel in high pressure before

passing the entrance aperture of the first lens element) [22]. Using Eq. 1 the intensity corrections terms (I_p/I_0) were found to be 0.214 for S 1s and 0.445 for Ti 2p.

Three observations from the spectra in Fig. 3 can be made. First, the dependence of spectral intensity on ambient pressure clearly shows that the gas attenuation effect is strong and cannot be neglected when comparing relative intensities between peaks whose kinetic energies largely differ. Second, Eq. 1 adequately corrects for attenuation effects, such that the intensity of the S 1s peak relative to the Ti 2p peak is recovered within the accuracy of the measurements. Third, the S 1s peak undergoes a small shift of 0.2 eV to higher binding energies upon water exposure. This may be interpreted as a change in the dye molecule electronic structure upon exposure to high pressures of water vapor. This change may be a result of a specific molecular reorganization of the ligand due to the presence of condensed water. Additional information about a possible structural change due to the presence of water can be obtained from the C 1s and Ru 3d spectra. The kinetic energies of the photoelectrons arising from Ti 2p, C 1s, and Ru 3d using 4000 eV photon energy are high and similar, and thus a significant difference in gas phase attenuation is not expected. A calculation according to Eq. 1 shows that the actual difference will be around 4 % between Ti 2p and C 1s when using a photon energy of 4000 eV, thus a negligible effect on the relative intensities of the spectra [42]. The spectra are shown in Fig. 4. In accordance with the intensity observation in the S 1s spectra, the intensity of the Ru 3d peak remains largely unaffected by water. The C 1s intensity increases slightly, probably due to contamination from the measurement chamber over time. Since the S 1s, C 1s, and Ru 3d intensities are mostly unaffected by the presence of water, the shift observed in the S 1s binding energy is likely caused by specific water adsorption at the dye molecules anchored on the TiO_2 surface.

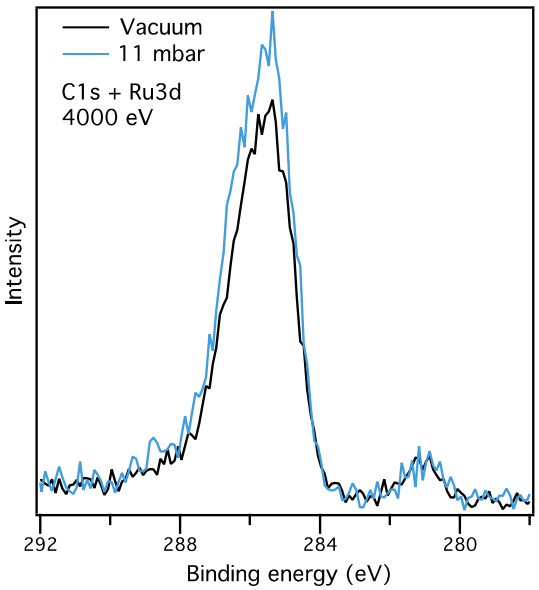

Fig. 4 C 1s and Ru 3d spectra of the dye-sensitized TiO_2 sample recorded in vacuum and at partial pressures of gaseous water of 11 mbar and excited with 4000 eV. The C 1s contribution is centered at 286 eV and Ru 3d at 281 eV. The spectra are intensity normalized to the corresponding Ti 2p peak intensity. The increase of the C 1s intensity is most likely due to contamination of the sample in the chamber

In a previous work on Z907 no change was observed of the sulfur signal (S 2p) due to water exposure [12]. The present results for the S 1s level are not, however, inconsistent with the previous results, since the experiments were performed under different conditions, in particular with respect to the presence of molecular water during the measurements. In the previous experiments the dye-sensitized TiO_2 surfaces were measured under high vacuum conditions after ex situ exposure to liquid water. In the present experiments, the electrodes were in situ exposed to water vapor and also measured in situ in the presence of water vapor.

In order to shed more light on the possible adsorption geometries of the water molecules at the dye-vacuum interface, model DFT calculations were made for the 4,4-diethyl-2,2-bipyridine analogue of Z907 including water molecules. The optimized geometries showed two hydrogen bonded adsorption sites as depicted in Fig. 5. For these geometries, the S 1s binding energies were calculated and compared to the bare dye molecule. As can be seen, one preferred adsorption geometry entails N–C–S–H–O–H–S–C–N hydrogen bonding bridging between the two thiocyanate groups of the dye, producing an increase of approximately 0.2 eV in the S 1s binding energy in accordance with our experimental observation. The other preferred adsorption geometry involves the anchoring carboxylate groups of the dye, leading to a somewhat smaller S 1s shift. This geometry, however, assumes that the water affects the anchoring of the dye to the TiO_2 substrate. There may be a significant probability for such an effect, but a more detailed analysis would require model calculations including also the substrate, which is beyond the scope of the present paper. It may be noted that no stable water adsorption sites were found on the 4,4-diethyl-2,2-bipyridine—ligand side of the molecule, which is in agreement with the expected hydrophobic character of this moiety.

Valence band spectra of Z907 adsorbed on TiO_2 measured at different partial pressures of gaseous water are shown in Fig. 6. The broad feature between 8 and 2 eV is dominated by the valence band of the TiO_2 and the small feature at the lowest binding energy is the HOMO level of the dye [9, 43]. The HOMO level is known to be a mixture of molecular orbitals from the NCS-ligand and Ru [44]. When probed with high energies (here 4000 eV), the relative contributions of the Ru 4d components to the HOMO level photoemission signal will dominate [44] due to the

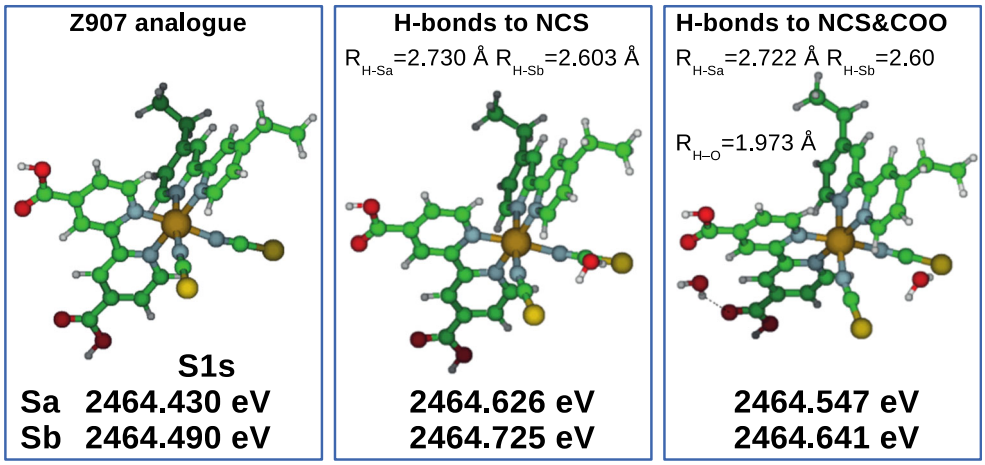

Fig. 5 Calculated S 1s binding energies for the free Z907 analogue (*left*), Z907 with one H_2O molecule hydrogen bonded to the NCS groups (*middle*) and Z907 with H_2O molecules hydrogen bonded to both the NCS groups and one of the COOH groups (*right*)

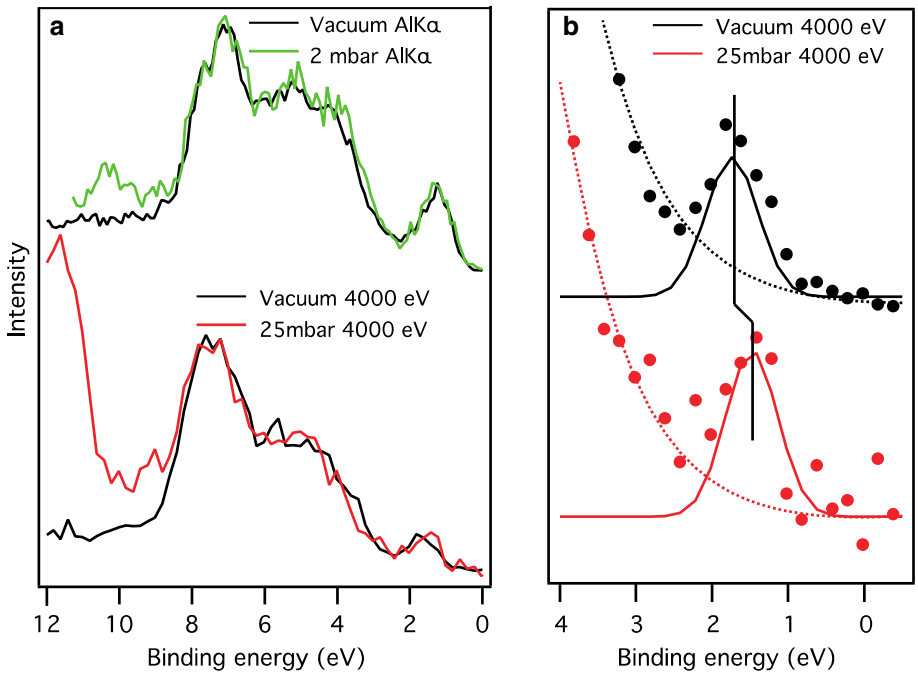

Fig. 6 **a** Upper spectra: the valence band of Z907 sensitized TiO_2 measured for different partial pressures of gaseous water with Al Kα radiation. The *black* spectrum is recorded in vacuum and the *green* in 2 mbar water vapor. The feature around 10 eV stems from gaseous water. Lower spectra: The valence band of Z907 sensitized TiO_2 measured with 4000 eV. The *black* spectrum is recorded in vacuum and the *red* spectrum in 25 mbar H_2O atmosphere. The feature around 12 eV stems from gaseous water. The broad feature between 8 and 2 eV is due to the semiconductor substrate. The peak around 1.5 eV is due to the HOMO level of the dye molecule. **b** The spectra indicate a shift of approximately 0.15 eV of the HOMO level when the sample is subject to 25 mbar water atmosphere

higher photoionization cross section for the d level compared to *p* levels of lighter elements. However, in the present experiments the possible effects of such a difference in relative sensitivity of the NCS and Ru contributions to the HOMO peak using 1486.58 eV (Al Kα) and 4000 eV photon energies could not be identified. At binding energies of around 10 and 12 eV, contributions from gas-phase water can be seen for the spectra recorded at 2 and 25 mbar, respectively [45]. The contributions from adsorbed water are expected to overlap with the valence band of TiO_2 and hence cannot be separately identified in the present spectra [46].

As seen in the upper part of Fig. 6a, there are no significant differences between the valence band spectra

obtained in vacuum and at water pressures of 2 mbar. When the pressure is increased to 25 mbar, however, there is a small but significant effect on the spectrum. Specifically, the HOMO level shifts about 0.15 eV to lower binding energy (see Fig. 6b) when the dye-sensitized sample is exposed to 25 mbar of water vapour.

A shift in the HOMO level of the dye molecule of 0.15 eV could have a significant influence on the solar cell performance, since the energy level alignment between the various cell components plays a significant role in the kinetics of charge transfer in the solar cell. Regeneration of the dye molecules by the electrolyte occurs through electron transfer from the electrolyte into the HOMO level of the dye. An increase in the HOMO level of the dye molecule, as indicated by our measurements, therefore reduces the driving force for regeneration and can slow down the rate of electron transfer from the electrolyte to the oxidized dye [47, 48]. A loss in photocurrent and a minor blueshift of the dye photoabsorption have been observed [5] in solar cells using hydrophobic dye molecules similar to Z907 and a water-based electrolyte. These results together with our observation of the shift in the HOMO level suggests that a similar but slightly larger shift occurs in the LUMO level. This could be further investigated by measuring the LUMO level with e.g. electrochemical methods, inverse photoemission spectroscopy, or X-ray absorption spectroscopy (XAS). Law et al. [5] mainly attribute the main loss of photocurrent to a reduced current carrying capability of the electrolyte in the electrode pores, however our present results, combining the core and valence level results with the theoretical calculations, indicate that the electrolyte/dye/TiO_2 interface is affected by the presence of water in specific adsorption sites. The study presented in this paper allows the effect of the solvent molecules on the active interface in the solar cell to be followed, thus complementing studies characterizing the function of dye sensitized solar cells.

4 Conclusions

AP-PES and AP-HAXPES have provided novel routes for investigating energy related photoelectrochemical systems in ambient conditions. In this paper, we present photoemission results of the Z907 sensitized TiO_2 solid surface in the presence of condensed water and/or gas-phase water. We have demonstrated that water is present in a condensed phase on a dye-sensitized TiO_2 substrate at a water vapor pressure of 25 mbar and thus that sufficient high ambient pressures of water molecules are required to create the relevant conditions akin to the real functional interface. The presence of water influences the chemical structure of the interface between the hydrophobic Z907 dye and the TiO_2 via the presence of specific water adsorption sites but does not influence the stoichiometry of the dye-molecule, as determined by the adopted quantitative AP-HAXPES analysis methodology. The results of this paper represent a first step towards in-operando measurements on complete photoelectrochemical interfaces in devices that include liquid electrolytes. It is to be expected that the further development of such measurements will be important aids in the continuing efforts for optimization of photoelectrochemical systems, such as DSCs.

Acknowledgments The friendly and helpful staff at Advanced Light Source is greatly acknowledged. ALS is supported by the Department of Energy, Basic Energy Sciences, Contract No. DE-AC02-05CH11231. The Swedish Energy Agency (P22191-5), the Swedish Research Council (VR-2010-4132, VR-2014-6019, VR-2015-03956), the STandUP-strategic research program and Carl Trygger Foundation (CTS 14:355) are acknowledged for funding. The HiPP-2 system was developed at VG Scienta AB with funding from Swedish Governmental Agency for Innovation Systems (VINNOVA). The theoretical modelling was made possible through generous allocations of computer time provided by the Swedish National Infrastructure for Computing (SNIC) at the Swedish National Supercomputer Center (NSC) and the High Performance Computer Center North (HPC2N). Furthermore, RGW, DES, and MB are grateful for the financial support of the Helmholtz-Association (VH-NG-423).

References

1. Cf. Fujishima A, Zhang X, Tryk DA (2008) Surface Science Reports 63:515–582 and references therein
2. Cf. Hagfeldt A, Boschloo G, Sun L, Kloo L, Pettersson H (2010) Chem Rev 110:6595–6663 and references therein
3. O'Regan B, Grätzel M (1991) Nature 353:737–740
4. Mathew S, Yella A, Gao P, Humphry-Baker R, Curchod BFE, Ashari-Astani N, Tavernelli I, Rothlisberger U, Nazeeruddin MK, Graetzel M (2014) Nat Chem 6:242–247
5. Law CH, Pathirana SC, Li XO, Anderson AY, Barnes PRF, Listorti A, Ghaddar TH, O'Regan BC (2010) Adv Mater 22:4505–4509
6. Daeneke T, Uemura Y, Duffy NW, Mozer AJ, Koumura N, Bach U, Spiccia L (2012) Adv Mater 24:1222–1225
7. Zakeeruddin SM, Nazeeruddin MK, Humphry-Baker R, Péchy P, Quagliotto P, Barolo C, Viscardi G, Grätzel M (2002) Langmuir 18:952–954
8. Murakami T, Saito H, Uegusa S, Kawashima N, Miyasaka T (2003) Chem Lett 32:1154–1155
9. Johansson EMJ, Hedlund M, Siegbahn H, Rensmo H (2005) J Phys Chem B 109:22256–22263
10. Johansson EMJ, Hedlund M, Odelius M, Siegbahn H, Rensmo H (2007) J Chem Phys 126:244303
11. Hahlin M, Odelius M, Magnuson M, Johansson EMJ, Plogmaker S, Hagberg DP, Sun LC, Siegbahn H, Rensmo H (2011) Phys Chem Chem Phys 13:3534–3546

12. Hahlin M, Johansson EMJ, Schölin R, Siegbahn H, Rensmo H (2011) J Phys Chem C 115:11996–12004
13. Schwanitz K, Weiler U, Hunger R, Mayer T, Jaegermann W (2007) J Chem Phys C 111:849–854
14. Josefsson I, Eriksson SK, Ottosson N, Ohrwall G, Siegbahn H, Hagfeldt A, Rensmo H, Bjorneholm O, Odelius M (2013) Phys Chem Chem Phys 15:20189–20196
15. Eriksson SK, Josefsson I, Ottosson N, Öhrwall G, Björneholm O, Siegbahn H, Hagfeldt A, Odelius M, Rensmo H (2014) J Phys Chem B 118:3164–3174
16. Bluhm H (2010) J Electron Spectrosc Relat Phenom 177:71–84
17. Starr DE, Liu Z, Havecker M, Knop-Gericke A, Bluhm H (2013) Chem Soc Rev 42:5833–5857
18. Liu X, Yang W, Liu Z (2014) Adv Mater 26:7710–7729
19. Gelius U, Basilier E, Svensson S, Bergmark T, Siegbahn K (1973) J Electron Spectrosc Relat Phenom 2:405–434
20. Siegbahn H, Svensson S, Lundholm M (1981) J Electron Spectrosc Relat Phenom 24:205–213
21. Siegbahn H, Lundholm M, Arbman M, Holmberg S (1984) Physica Scripta 30:305–308
22. Ogletree DF, Bluhm H, Lebedev G, Fadley CS, Hussain Z, Salmeron M (2002) Rev Sci Instrum 73:3872–3877
23. Salmeron M, Schlogl R (2008) Surf Sci Rep 63:169–199
24. Grass ME, Karlsson PG, Aksoy F, Lundqvist M, Wannberg B, Mun BS, Hussain Z, Liu Z (2010) Rev Sci Instrum 81:053106
25. Schnadt J, Knudsen J, Andersen JN, Siegbahn H, Pietzsch A, Hennies F, Johansson N, Martensson N, Ohrwall G, Bahr S, Mahl S, Schaff O (2012) J Synchrotron Radiat 19:701–704
26. Brown MA, Redondo AB, Jordan I, Duyckaerts N, Lee M-T, Ammann M, Nolting F, Kleibert A, Huthwelker T, Mächler J-P, Birrer M, Honegger J, Wetter R, Wörner HJ, van Bokhoven JA (2013) Rev Sci Instrum 84:073904
27. Mangolini F, Ahlund J, Wabiszewski GE, Adiga VP, Egberts P, Streller F, Backlund K, Karlsson PG, Wannberg B, Carpick RW (2012) Rev Sci Instrum 83:093112
28. Eriksson SK, Hahlin M, Kahk JM, Villar-Garcia IJ, Webb MJ, Grennberg H, Yakimova R, Rensmo H, Edström K, Hagfeldt A, Siegbahn H, Edwards MOM, Karlsson PG, Backlund K, Ahlund J, Payne DJ (2014) Rev Sci Instrum 85:075119
29. Edwards MOM, Karlsson PG, Eriksson SK, Hahlin M, Siegbahn H, Rensmo H, Kahk M, Villar Garcia IJ, Payne DJ, Åhlund J, Nucl Inst Methods Phys Res A. doi:10.1016/j.nima.2015.02.047
30. Perera R, Jones G, Lindle D (1994) Review of Scientific Instruments 1995, 66, 1745–1747. In: 5th International Conference on Synchrotron Radiation Instrumentation, Stony Brook, NY, 18–22 July 1994
31. Axnanda S, Crumlin E, Mao B, Rani S, Chang R, Karlsson P, Edwards M, Lundqvist M, Moberg R, Ross P, Husssain Z, Liu Z (2015) Sci Rep 5:9788
32. Gaussian 09, Revision D.01, Frisch MJ et al., Gaussian, Inc., Wallingford CT, 2013
33. Becke AD (1993) J Chem Phys 98:5648–5652
34. Wadt WR, Hay PJ (1985) J Chem Phys. 82:284–298
35. Dunning TH Jr, Hay PJ (1977) In: Schaefer HF (ed) Modern theoretical chemistry, vol 3. Plenum, New York, pp 1–28
36. Hermann K, Pettersson LGM, Casida ME, Daul C, Goursot A, Koester A, Proynov E, St-Amant A, Salahub, DR, Contributing authors: Carravetta V, Duarte H, Friedrich C, Godbout N, Guan J, Jamorski C, Leboeuf M, Leetmaa M, Nyberg M, Patchkovskii S, Pedocchi L, Sim F, Triguero L, Vela A (2013) StoBe-deMon version 3.2
37. Becke AD (1988) Phys Rev A 38:3098
38. Perdew JP, Wang Y (1986) Phys Rev B 33:8800
39. Kutzelnigg W, Fleischer U, Schindler M (1990) Al–Cl: The IGLO-method: ab initio calculation and interpretation of NMR chemical shifts and magnetic susceptibilities. Springer, Heidelberg, p 23
40. Godbout N, Salahub DR, Andzelm J, Wimmer E (1992) Can J Chem 70:560
41. Almlof M, Kristensen EME, Siegbahn H, Aqvist J (2008) Biomaterials 29:4463–4469
42. Munoz A, Oller JC, Blanco F, Gorfinkiel JD, Limao-Vieira P, Garcia G (2007) Phys Rev A 76:052707
43. Johansson EMJ, Edvinsson T, Odelius M, Hagberg DP, Sun LH, Hagfeldt A, Siegbahn H, Rensmo H (2007) J Phys Chem C 111:8580–8586
44. Johansson EMJ, Odelius M, Gorgoi M, Karis O, Ovsyannikov R, Schafers F, Svensson S, Siegbahn H, Rensmo H (2008) Chem Phys Lett 464:192–197
45. Kimura K (1981) Handbook of HeI photoelectronspectra of fundamental organic molecules. Japan Scientific Societies Press, Tokyo, p 268
46. Martensson N, Malmquist P, Svensson S, Basilier E, Pireaux J, Gelius U, Siegbahn K (1977) New J Chem 1:191–195
47. Listorti A, O'Regan B, Durrant JR (2011) Chem Mater 23:3381–3399
48. Ardo S, Meyer GJ (2009) Chem Soc Rev 38:115–164